www.nesa-india.org • E-mail: nesapublications@gmail.com
International Journal on Environmental Sciences

International Journal on Environmental Sciences 13 (2) Pp. 99-106, ***July-December 2022***
ISSN No.: 0976-4534
https://doi.org/10.53390/ijes.v13i2.6

ANALYZING THE IMPACT OF BUILT UP AND GREEN SPACES ON LANDSURFACE TEMPERATURE WITH SATELLITE IMAGES IN JALANDHAR SMART CITY

Yukti Prashar[1], Reenu Sharma[1], Sumit Kumar[1], Syed Shabih Hassan[2] and Brijendra Pateriya[1]

[1]Punjab Remote Sensing Centre, Ludhiana-141004 (Punjab) India
[2]College of Fisheries, Guru Angad Dev Veterinary and Animal Sciences University Ludhiana-141004 (Punjab) India

Research Article

Received: **10.09.2022** Accepted: **22.09.2022** Published: **02.10.2022**

ABSTRACT

Land use in developing nations is shifting as a result of rapid urbanisation. The ecosystem is being harmed by the unplanned, urban development of cities. Utilizing data from Landsat, the present research examined the spatiotemporal urban growth in Jalandhar City and its impact on variations in land surface temperature (LST). The results indicate that urban regions have increased while urban green spaces have shrunk (UGS). UGS and LST have been found to be inversely correlated. Where there was a low percentage of urban areas and a high percentage of accessible green spaces, it was observed that the LST decreased. The link between spectral variability and changes in vegetation growth rate was studied using the NDVI (Normalized Difference Vegetation Index). It works on tracking the growth of green vegetation and spotting variations in the amount of greenery. Where NDVI value was low, the scatter plots indicate higher surface temperatures. The dense urban regions with little available vegetation cover were linked to the low NDVI number and the NDVI is negative in the urban area of Jalandhar. High NDVI values indicate regions with dense vegetation and low surface temperatures. The research findings of present study could be applied to urban administration, planning, management and research projects.

Keywords: LST, NDVI, Urban Expansion, Urban Green Spaces, Urban Heat Island, Landsat.

INTRODUCTION

On a global scale, urban regions currently reside 56.2 percent of the population. According to the UN-Habitat World Cities study, the future population growth will be concentrated in cities. From 2018 to 2050, about 35% of predicted urban population growth will be centered in India, China, and Nigeria – In India, the metropolitan cities, urban centers, and expanding urban infrastructures are increasingly subject to aggressive urbanization . This increasing urban area in the cities can be defined as Urban Sprawl ' . It is characterized by single-use, scattered low-density residential areas due to planned or unplanned urban development. The unplanned urban sprawl leads to high carbon emissions, reduction in green spaces and poor infrastructural development — . These expanding urban zones are responsible for transforming natural surfaces into urban areas, affecting evapo-transpiration, albedo, surface emissivity; anthropogenic heat flow, wind speed, and air pollution, among other physical and biophysical features – . Changes in these characteristics can change the local and regional climate in the long run .

Urban Heat Islands (UHI) are the most visible example of local climate alteration caused by urbanization ' . Urban areas have higher temperatures than non-urban areas. This phenomenon leads to the difference between urban and rural temperatures. The intensity of UHI is primarily determined

*Corresponding author: *reenusharma30@gmail.com; reenusharma@prsc.gov.in*

by the urban geometry and the capacity of the urban fabric to absorb heat . UHI occurs when natural green areas are replaced with grey surfaces (concrete). The impervious and concrete surface absorbs incoming solar radiation and increases the surface temperature . This UHI can directly impact city dwellers' thermal comfort and health. Additionally, UHI has been linked to increased energy demand for cooling, increased day and night temperature, and heat-related mortality and sickness. Remote sensing data has been extensively used to analyze LST in relation to green spaces and built-up areas. Landsat data has been widely used for the retrieval of LST due to its long time series archive ' . The Landsat data provides high-resolution thermal data making it fit for analyzing local or city level studies '—' . This study aims to use remote sensing data to examine urban expansion and its effects on surface temperature. The objectives of this study were (i) Time Series land use land cover analysis of Jalandhar city from 2000 to 2020. (ii) Spatial pattern and correlation of NDVI and LST.

1. MATERIAL AND METHODS

2.1. Study area

Jalandhar city lies in the north-eastern part of Punjab (India), located between 35°59´ and 31°37´ N latitudes and 75°04´ and 75°57´E longitudes and it covers area around 99.79 km² in (Fig.1).The city is part of the Trans-Indian Ganges Plain, the terrain is almost flat, and the area's soil is very fertile. The climate of Jalandhar can be classified as tropical and dry sub-humid. The maximum temperature varies from 19.4°C in January and 40°C May and June. The average annual rainfall in the area was about 569 mm. Maximum precipitations is obtained from the southwest monsoon.The Jalandhar city is developing as important industrial and commercial hub in India . The detailed methodology chart has been shown in (F i g . 2) .

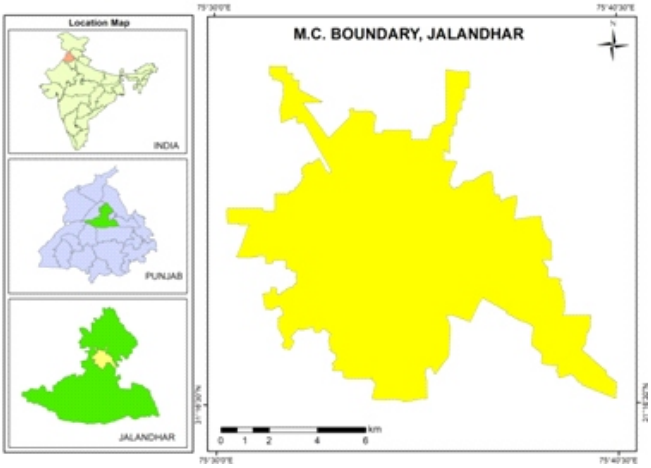

Fig. 1:Study area map of Jalandhar city.

2.2. Satellite data and image pre-processing

The Landsat data were was used in this study, including Landsat 5 Thematic Mapper (TM) and Landsat 8 Operational Land Imager (OLI) satellite images. These images were downloaded from the United States Geological Survey (USGS) Earth Explorer site of 2000, 2010 and 2020. Landsat 5 (TM) provides spectral information in seven bands: band 1, 2 and 3 (blue, green and red) obtained in the visible range, band 4 in the Near Infrared (NIR) and band 6 is a thermal infrared band (TIR) with 120 m spatial resolution. Landsat 8 (OLI) acquires the images in 11 spectral bands: band 2, 3 and 4 (blue, green and red) in visible range, band 5(NIR) and 10 and 11 (TIRS) thermal infrared bands) with 100 m spatial resolution while other bands with 30m spatial resolution. The remote sensing images were first pre-processed for atmospheric correction. There after Layers stacking, and image subset were undertaken.

2.3. Land Use Land Cover Classification and Change Analysis

Many Studies reviewed to select the best and most appropriate classification method in which supervised classification methods have been widely used —— (Adam et al., 2014; Bokaie et al., 2016; Kaul & Sopan, 2012; Shahtahmassebi et al., 2021; Talukdar et al., 2020).The pre-processed images were used as inputs in image classification. The maximum likelihood classifier has been used for the land use land cover classification. The training sample collected for the classification were spread around the whole image and pure classes were selected. These training samples provides variability within the class and between the other classes. In the classification, two classes' i.e.,built-up and non-built-up or green spaces were selected for LULC classification. The output results land cover changes and time series variations were studied for Jalandhar.

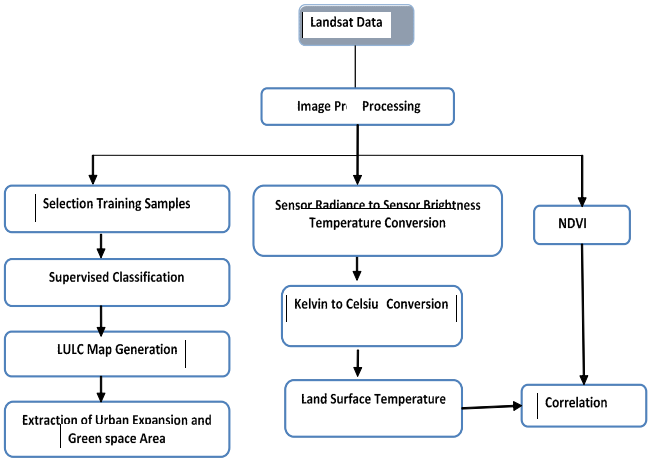

Fig. 2: Methodological approach used in this study

2.4. Derivation of Land Surface Temperature

The Landsat 5(TM) band 6 and Landsat 8 (OLI) band 10 were used to retrieve Land surface temperature.

LST estimation for Landsat 5:

For the mapping of land surface temperature from Landsat 5 data following steps were followed: (1) conversion of Digital number into the spectral radiance (2) converting the spectral radiance to temperature (Kelvin scale) image; and (3) converting the temperature in Kelvin to degree Celsius.

Step 1: Covert top of Atmospheric digital number to spectral radiance calculation formula for Landsat 5 data:

(1) $$L(\lambda) = Lmin(\lambda) + \frac{(Lmax(\lambda) - Lmin(\lambda))Qdn}{Qmax}$$

Where: L(λ) spectral radiance, Lmin (λ) minimum spectral radiance, L max (λ) maximum spectral radiance, Q dn= gray level of the TM image (DN= 0), Qmax=maximum numerical value of the TM image (Q max= 255) equation (1).

Step2: Conversion of spectral radiance to Temperature in Kelvin

(2) $$T\mathrm{B} = K2/\{\left(\frac{K1}{L\lambda}\right) + 1\}$$

(Alhawiti & Mitsova et al., 2016) provides the formula to converts the spectral radiance to at satellite brightness temperature equation (2), where:

TB is the satellite brightness temperature in degree Kelvin; K1 and K2 are the pre-calibration constants of thermal band from the metadata file (Downloaded from USGS), the value of K1 = 607.76 and K2 = 1260.56 for Landsat 5 thermal band.

Step 3: Conversion of Kelvin to Celsius

$$T\mathrm{B} = T\mathrm{B} - 273 \quad (3)$$

LST estimation for Landsat 8:

For the mapping of land surface temperature from Landsat 8 data following steps were followed: (1) conversion of Digital number into the spectral radiance (2) converting the spectral radiance to temperature (Kelvin scale) image; and (3) NDVI Calculation (4) Emissivity Calculation (5) Derivation of LST.

The brightness temperature Tb is determined using radiative transfer equations, which estimate top of the atmosphere (TOA) radiances and use Planck's law to calculate blackbody temperatures equation (1).Landsat 8 has two thermal bands (band 10 and 11), but the only band 10 is used in the LST calculation due to uncertainty in the bands 11 .

Step 1: Covert top of Atmospheric digital number to spectral radiance calculation formula for Landsat 8 data:

(1) $$L(\lambda) = \mathrm{ML} * \mathrm{QCAL} + \mathrm{AL}$$

Where:

L (λ) = Top-of-Atmosphere (TOA) spectral radiance in W/ (m2.sr.mm), ML = Band-specific multivariate rescaling factor from the metadata, AL = band-specific additive rescaling factor from the metadata, Qcali= Calibrated standard product pixel value (DN) Oi: i= Offset used for the calibration of Landsat 8 TIRS band.

Step 2: The next step was to convert the spectral radiance into brightness temperature.

The satellite brightness temperature TB in degree Kelvin; K1 and K2 are the pre-calibration constants of thermal band from the metadata file (Downloaded from USGS), the value of K1 = 774.8853 and K2 = 1321.0789 for Landsat 8, band 10 equation (2).

$$T\mathrm{B} = \frac{K2}{\left\{\left(\frac{K1}{L1}\right)+1\right\}} - 273.15 \quad (2)$$

Step 3: NDVI calculation

Emissivity is calculated using the NDVI threshold approach, which used OLI bands 4 and 5.

The NDVI is a useful indication of vegetative stress, health, greenness, andbiomass. NDVI values ranged from - 1 to + 1 and positive values indicated vegetation, while negative values represented barren areas containing no vegetative cover equation (3).

The Normalized Difference Vegetation Index (NDVI) calculation formula:

$$\mathrm{NDVI} = (\mathrm{NIR} - \mathrm{RED}) / (\mathrm{NIR} + \mathrm{RED})$$

Step 4: Emissivity Calculation

In this study, for estimation of LST, we have used the method (Dar et al., 2019) that considered variance (m), alongside soil and vegetation emissivity (n), and the proportion of vegetation (PV) as calculated from equations (4),(5) and (6).Obtain the land surface emissivity (e) from equation (7).

$$m = (\varepsilon v - \epsilon s) - (1 - \epsilon s) F \varepsilon v \quad (4)$$

$$n = \epsilon s (1 - \epsilon s) F \varepsilon v \quad (5)$$

$$Pv = \left(\frac{NDVImin}{NDVImax} - NDVImin\right)^2 \quad (6)$$

$$\varepsilon = mPv + n \quad (7)$$

Where, ∈ Sand εv are the soil and vegetation emissivity, F=0.55 (shape factor and it considering different geometric distribution ' We have considered m= 0.004 and n=0.986 these findings of ' .

Step 5: Derivation of LST

Finally, LST were calculated from Landsat 8 TIRS band 10 using equation (8), at satellite brightness temperature (TB) obtained from equation (3) and the corrected for surface emissivity (e) from equation (7)and in last temperature converted to degree Celsius (°C) equation (8).

$$LST = TB =/ (1 + (\lambda TB/\rho)\ln \varepsilon \quad (8)$$

Where (λ) wavelength of emitted radiance (λ=10.8 m) for band 10 of Landsat 8 (Dar et al., 2019).

$$\rho = h * c/\sigma(1.438 * 1010^{-2}mk)$$
$$\sigma = \text{Boltzmann constant } (1.38*10^{-23}J/K)$$
$$h = \text{Planck's constant } (6.625 * 10^{-34}Js)$$
$$c = \text{velocity of light } (2.998 * 10^{8}m/s)$$
$$\varepsilon = \text{land surface emissivity}$$

2.5. Statistical analysis and spatial analysis

Pearson's correlation coefficient was used to analyze the linear correlation between LST and NDVI. The correlation coefficient was used to measure the relationship. The statistical method depends on the properties of the variable or the scale of the variable. There is a medium to high relationship if the correlation coefficient value is 1 or close to 1. Conversely, if the value is close to 0, there is a medium-low relationship or no relationship. In addition, the positive or negative sign in mathematics indicates the direction of the relationship. The plus sign represents the value of the positive relationship and the minus sign represents the value of the negative relationship in equation (9).

$$r_{xy} = \sum_{i=1}^{n} \frac{(xi - x)(yi - y)}{\sqrt{\sum_{i=1}^{n}(xi - x)^2}\sqrt{\sum_{i=1}^{n}(yi - y)^2}} \quad (9)$$

The correlation analysis has been carried out to understand the relationship between of LST and NDVI. The scatter plots of LST and NDVI have been generated to draw the trend line and statistically analyses of the degree of effect and relationship, R^2 values were calculated.

3. RESULTS AND DISCUSSION

3.1. Land Use Land Cover changes in 2000, 2010 and 2020

The results show that Jalandhar city has experienced rising urbanizations from 2000 to 2020 (Fig. 3, 4, 5 and Table 1). The LULC classification shows a substantial change in the urban area. The total built-up area in 2000 was 73.38 km², it increased to 78.92 km² by 2010 and finally reached 87.21 km² in 2020. It was observed that from 2000 to 2020, the transition takes place in which a large quantity of fallow land and empty land was converted into an urban area and followed by plantation, cropland and vegetation. The amount of this conversion was high for the sites that contain green cover. The change of fallow land and empty regions to urban areas increased considerably.

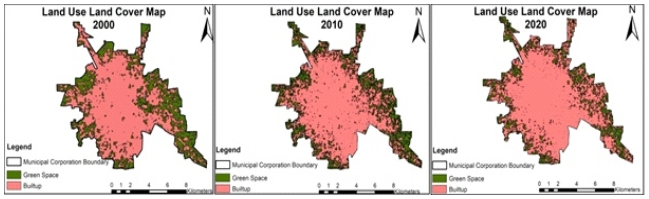

Fig.3 : LULC Maps of Jalandhar City during 2000, 2010 and 2020.

The results demonstrate that a significant area of 28.76 km² (2000), 20.35 km² (2010) and 14.40 km²of cropland have been converted to urban space. The change in land use/cover was mostly caused by over exploitation of land for built-up purposes and to raise real estate value.

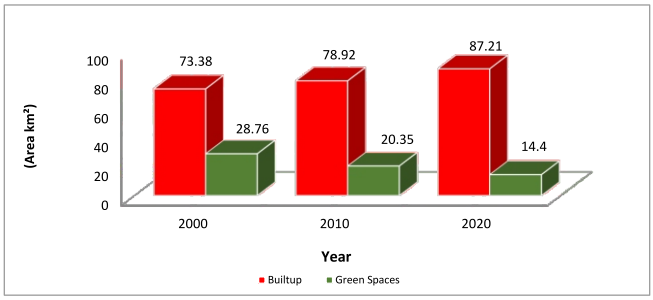

Fig. 4 : Area statistics analysis of urban expansion and urban green spaces.

Table 1: Urban growth and green spaces statistics of Jalandhar city during 2000 to 2020.

Year	Increase in Built-up area (km²)	Decrease in green spaces area (km²)
2000 -2010	5.54	8.41
2010- 2020	8.29	5.95

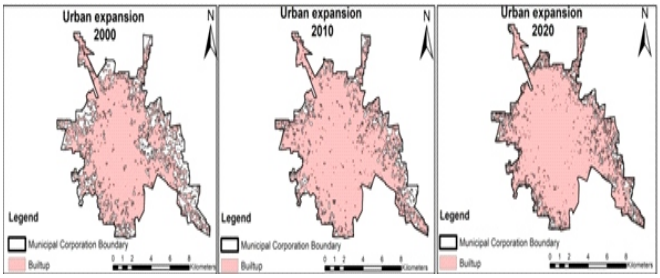

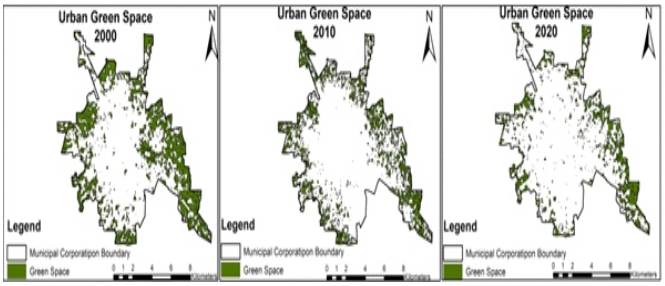

Fig. 5: Spatial temporal changes in urban expansion and urban green spaces during 2000, 2010 and 2020.

3.2. Spatial Pattern of Normalized Difference Vegetation Index

The NDVI have been broadly used to study the relationship between spectral variability and changes in vegetation growth rate. It is also effective for determining the development of green vegetation and detecting changes in green cover. For the respective years in NDVI most remarkable change was found. NDVI in Jalandhar city varies the range of NDVI values in 2000 from -0.14 to 0.51, in 2010 -0.11 to 0.49 and in 2020 image from -0.02 to 0.56 (Fig.6). The positive NDVI value shows the high green cover, while lower NDVI value shows the barren and urban areas. The green areas in Jalandhar are situated in the north and west direction of the city. The NDVI value was highest in the dense vegetation area of the outer edge. Furthermore, in 2000 and 2010, the NDVI values ranges are higher than 2020, which shows that the density of vegetation in Jalandhar has been more than in 2020.The NDVI is mostly negative in the urban area.

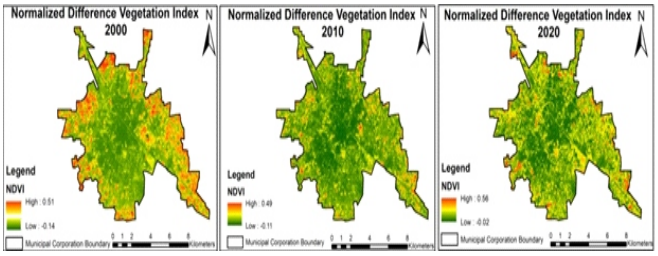

Fig.6 : Normalized difference vegetation index (NDVI) of Jalandhar City 2000, 2010 and 2020.

3.3. Spatial Pattern of Land Surface Temperature

The distribution of LST shows that the city has more temperature inside than its outskirts (Fig.7). The LST distribution in Jalandhar city depicts a change in the surface temperatures in time series. The temperature varies from of 36.05 °C (May) in the year 2000, followed by 42.96 °C (June) in 2010, and then, it was 49.39 °C (June) in 2020, whereas the minimum temperature was observed to be 20.64 °C in 2000, 30.42 ° in 2010 and 33.12 ° in 2020 and the average LST in the study area was 28.20°C, 37.82°C and 43.03°C in from 2000 to 2020 (Table 2).

Table 2: The statistical information of the land surface temperature.

Date	Minimum temperature	Average temperature	Maximum temperature
May 2000	21.64	28.20	34.52
June 2010	32.05	37.82	42.58
June 2020	33.73	43.03	48.25

The 30 years trend shows that LST is increasing which may cause of UHI effects. LST increases especially in the North and Northwestern part of the study area. This area consists of industrial center, center of economic and transportation. The distribution of LST can be influenced by the composition and structure of urban green spaces. The central part of the city consists of high-density residential area causing high surface temperature. The result showed that in 2000, 2010 and 2020 LST is increased.

Fig.7 : LST variation in Jalandhar City 2000, 2010 and 2020.

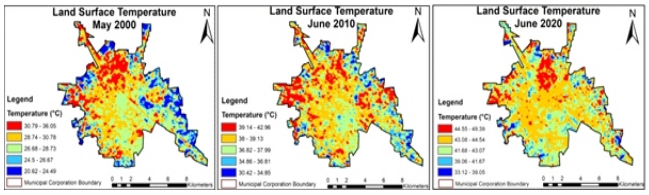

3.4. Correlation between Land Surface Temperature and Urban Green Spaces

The mean LST and NDVI shown negative correlation (Fig.8) respectively. The scatter plots shows higher surface temperature, where value of NDVI was low. The low value of NDVI was associated with the dense urban areas containing very low vegetation cover available. High value of NDVI shows high vegetative cover and these areas shows low surface temperature.

Fig.8: Correlation between LST and NDVI during 2000, 2010 and 2020.

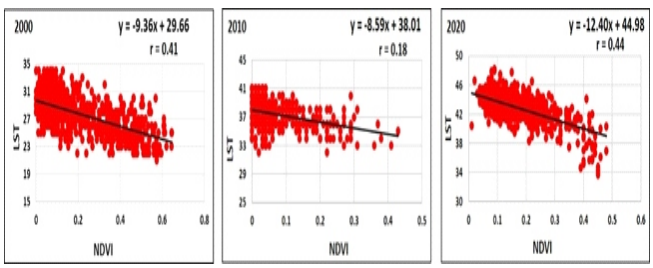

CONCLUSION

This study provides an analysis of LST in Jalandhar City using Landsat 5 TM and Landsat 8 OLI data from 2000 to 2020. The relationship between built-up area and Urban Green Space was studied, and their impact on Land Surface temperature was analyzed. The results clearly indicate that the Land surface temperature rises as the percentage of built-up land increases. The green cover in the city negatively impacts the Land surface temperature. The study suggested that the sustainable development of a city requires an adequate green surface, which helps to dissipate the solar energy into the environment and helps the urban areas reduce the temperature gradient. For the already developed regions, the use of trace gardening and a green roof will help to reduce the effect of the urban heat island. This study demonstrates that green spaces are essential for the urban environment to reduce negative impacts of urban sprawl.

ACKNOWLEDGEMENT

We gratefully acknowledge the United States Geological Survey Earth Explorer (USGS) and National Aeronautics and Space Administration (NASA) for providing open access Landsat data.

DECLARATION OF CONFLICTING INTERESTS

The authors declared no potential conflicts of interest with respect to the research, authorship and publication of this article.

REFERENCES

1. **Adam, G., Hermawan, R., Prasetyo, L. B., Rosli, A. Z., Reba, N. M., Roslan, N., & Room, M. H. M.** (2014). IOP Conference Series: Earth and Environmental Science Sustainable Urban Forestry Potential Based Quantitative And Qualitative Measurement Using Geospatial Technique You may also like Use of Geographical Information System (GIS) and remote sensing in development of urban forest types and shapes in Tangerang Selatan City Sustainable Urban Forestry Potential Based Quantitative And Qualitative Measurement Using Geospatial Technique. IOP Conf. Ser.: Earth Environ. Sci, 18, 12021. https://doi.org/10.1088/1755-1315/18/1/012021.
2. **Alhawiti, R.H. and Mitsova, D.** (2016). Using Landsat-8 Data to Explore the Correlation Between Urban Heat Island and Urban Land Uses. IJRET: International Journal of Research in Engineering and Technology, 5(3), pp.457-466.
3. **Beamish, A., Raynolds, M. K., Epstein, H., Frost, G. V., Macander, M. J., Bergstedt, H., Bartsch, A., Kruse, S., Miles, V., Tanis, C. M., Heim, B., Fuchs, M., Chabrillat, S., Shevtsova, I., Verdonen, M., & Wagner, J.** (2020). Recent Trends and Remaining Challenges for Optical Remote Sensing of Arctic Tundra Vegetation: A Review and Outlook. *Remote Sensing of Environment*, 246(March), 111872. https://doi.org/10.1016/j.rse.2020.111872.
4. **Bokaie, M., Zarkesh, M. K., Arasteh, P. D., & Hosseini, A.** (2016). Assessment of Urban Heat Island Based on the Relationship between Land Surface Temperature and Land Use/ Land Cover in Tehran. *Sustainable Cities and Society*, 23, 94–104. https://doi.org/10.1016/j.scs.2016.03.009.
5. **Dar, I., Qadir, J., & Shukla, A.** (2019). Estimation of LST from Multi-Sensor Thermal Remote Sensing Data and Evaluating the Influence of Sensor Characteristics. *Annals of GIS*, 25(3), 263–281. https://doi.org/10.1080/19475683.2019.1623318.
6. **Fuladlu, K., Riza, M., & Ilkan, M.** (2021). Monitoring Urban Sprawl Using Time-Series Data: Famagusta Region of Northern Cyprus. SAGE Open, 11(2). https://doi.org/10.1177/21582440211007465.
7. **Guan, K.** (2011). Surface and Ambient Air Temperatures Associated with Different Ground Material: A Case Study at the University of California, Berkeley. Surface and Air Temperatures of Ground Material, 14. http://nature.berkeley.edu/ classes/es196/ projects/2011final/GuanK_2011.pdf.
8. **Guo, J., Ren, H., Zheng, Y., Lu, S., & Dong, J.** (2020). Evaluation of Land Surface Temperature Retrieval from Landsat 8/TIRS Images Before and After Stray Light Correction Using the SURFRAD dataset. *Remote Sensing*, 12(6). https://doi.org/10.3390/rs12061023.
9. **He, X., Wang, J., Feng, J., Yan, Z., Miao, S., Zhang, Y., & Xia, J.** (2020). Observational and Modeling Study of Interactions between Urban Heat Island and Heatwave in Beijing. *Journal of Cleaner Production*, 247, 119169. https://doi.org/10.1016/j.jclepro.2019.119169.
10. **Kaul, H. a, & Sopan, I.** (2012). Land Use Land Cover Classification and Change Detection Using High Resolution Temporal Satellite Data. *Journal of Environment*, 01(04), 146–152.
11. **Khamchiangta, D., & Dhakal, S.** (2020). Time Series Analysis of Land Use and Land Cover Changes Related to Urban Heat Island Intensity: Case of Bangkok Metropolitan Area in Thailand. *Journal of Urban Management*, 9(4), 383–395. https://doi.org/10.1016/j.jum.2020.09.001.

12. **Kumar, R., Mishra, V., Buzan, J., Kumar, R., Shindell, D., & Huber, M.** (2017). Dominant control of Agriculture and Irrigation on Urban Heat Island in India. Scientific Reports, 7(1), 1–10. https://doi.org/10.1038/s41598-017-14213-2.

14. **Kurihara, Y., Murakami, H., Ogata, K., & Kachi, M.** (2021). A Quasi-physical Sea Surface Temperature Method for the Split-window Data from the Second-Generation Global Imager (SGLI) Onboard the Global Change Observation Mission-Climate (GCOM-C) Satellite. Remote Sensing of Environment, 257(January), 112347. https://doi.org/ 10.1016/j.rse.2021.112347.

15. **Piyoosh, A. K., & Ghosh, S. K.** (2022). Analysis of Land Use Land Cover Change using a New and Existing Spectral Indices and its Impact on Normalized Land Surface Temperature. Geocarto International, 37(8), 2137–2159. https://doi.org/10.1080/ 10106049.2020.1815863.

16. **Rahman, M. H., Islam, M. H., & Neema, M. N.** (2022). GIS-based Compactness Measurement of Urban form at Neighborhood Scale: The Case of Dhaka, Bangladesh. *Journal of Urban Management*, 11(1), 6–22. https://doi.org/10.1016/j.jum.2021.08.005.

17. **Ryu, Y. H., & Baik, J. J.** (2012). Quantitative Analysis of Factors Contributing to Urban Heat Island Intensity. *Journal of Applied Meteorology and Climatology*, 51(5), 842–854. https://doi.org/10.1175/JAMC-D-11-098.1.

18. **Salathé, E. P., Leung, L. R., Qian, Y., & Zhang, Y.** (2010). Regional Climate Model Projections for the State of Washington. *Climatic Change*, 102(1–2), 51–75. https://doi.org/10.1007/s10584-010-9849-y.

19. **Shahtahmassebi, A. R., Li, C., Fan, Y., Wu, Y., Lin, Y., Gan, M., Wang, K., Malik, A., & Blackburn, G. A.** (2021). Remote Sensing of Urban Green Spaces: A Review. *Urban Forestry & Urban Greening*, 57, 126946. https://doi.org/10.1016/j.ufug.2020.126946.

20. **Sholihah, R. I., & Shibata, S.** (2019). Retrieving Spatial Variation of Land Surface Temperature Based on Landsat OLI/TIRS: A Case of Southern Part of Jember, Java, Indonesia. IOP Conference Series: Earth and Environmental Science, 362(1). https://doi.org/ 10.1088/1755-1315/362/1/012125.

21. **Singh, H., Suryawanshi, S., & Planner, U.** (2019). Directional Change Detection of Urban Sprawling in Jalandhar City. *Global Journal of Engineering Science and Researches*., 6(May), 481–504.

22. **Singh, R., & Kalota, D.** (2019). Urban Sprawl and Its Impact on Generation of Urban Heat Island: A Case Study of Ludhiana City. *Journal of the Indian Society of Remote Sensing*, 47(9), 1567–1576. https://doi.org/ 10.1007/s12524-019-00994-8.

23. **Sun, L., Chen, J., Li, Q., & Huang, D.** (2020). Dramatic Uneven Urbanization of Large Cities Throughout the World in Recent Decades. *Nature Communications*, 11(1). https://doi.org/10.1038/s41467-020-19158-1.

24. **Sun, X., Liu, Y., Sun, T., Yu, S., Li, C., & Zhai, L.** (2021). Land Cover Changes and Urban Expansion in Chongqing, China: A Study Based on Remote Sensing Images. *Environment and Urbanization ASIA*, 12(1_suppl), S39–S58. https://doi.org/ 10.1177/0975425321998035.

25. **Talukdar, S., Singha, P., Mahato, S., Shahfahad, Pal, S., Liou, Y.-A., & Rahman, A.** (2020). Land-Use Land-Cover Classification by Machine Learning Classifiers for Satellite Observations—A Review. Remote Sensing, 12(7), 1135. https://doi.org/10.3390/rs12071135.

26. **Vinayak, B., Lee, H. S., Gedam, S., & Latha, R.** (2022). Impacts of Future Urbanization on Urban Microclimate and Thermal Comfort Over the Mumbai Metropolitan Region, India. *Sustainable Cities and Society*, 79(April 2021), 103703. https://doi.org/ 10.1016/j.scs.2022.103703.

27. **Vivekananda, G. N., Swathi, R., & Sujith, A. V. L. N.** (2021). Multi-Temporal Image Analysis for LULC Classification and Change Detection. *European Journal of Remote Sensing*, 54(sup2), 189–199. https://doi.org/10.1080/22797254.2020.1771215.

28. **Wamukoya, M., Kadengye, D. T., Iddi, S., & Chikozho, C.** (2020). The Nairobi Urban Health and Demographic Surveillance of Slum Dwellers, 2002–2019: Value, Processes, and Challenges. *Global Epidemiology*, 2, 100024. https://doi.org/ 10.1016/j.gloepi.2020.100024.

29. **Wang, J., Huang, B., Fu, D., Atkinson, P. M., & Zhang, X.** (2016). Response of Urban Heat Island to Future Urban Expansion Over the Beijing-Tianjin-Hebei Metropolitan Area. *Applied Geography*, 70, 26–36. https://doi.org/10.1016/j.apgeog.2016.02.010.

30. **Zhang, X. Q.** (2016). The Trends, Promises and Challenges of Urbanisation in the World. *Habitat International*, 54, 241–252. https://doi.org/ 10.1016/J.HABITATINT.2015.11.018.

Abbrevation Used

1. LST: Land Surface Temperature
2. TOA: Top of the Atmosphere
3. TB: Brightness Temperature
4. NDVI: Normalized Difference Vegetation Index
5. OLI: Operational Land Imager
6. PV: Proportion of Vegetation

7. UGS: Urban Green Space
8. UHI: Urban Heat Island
9. TIR: Thermal Infrared Band
10. USGS: United States Geological Survey
11. LULC: Land Use Land Cover
12. TM: Thematic Mapper